Chitosan/Alginate-loaded Astragalus hamosus shows ameliorating effects on lipid profile, inflammatory and hormonal parameters, and reduces miRNA-222 expression in Polycystic Ovary Syndrome Rats

Rashid Jafardoust Bostani
Islamic Azad University
Maryam Parvini Kohnehshahri
parvini29@gmail.com
Islamic Azad University
Zohreh Ghazi Tabatabaei
Islamic Azad University
Ata Pouryaee
Islamic Azad University

Research Article

Keywords: Polycystic ovary syndrome, Astragalus hamosus, Histopathological study, lipid profile, sex hormons, inflammatory parameters, miRNA 222, Rat

Posted Date: January 29th, 2024

DOI: https://doi.org/10.21203/rs.3.rs-3893640/v1

Additional Declarations: No competing interests reported.

Abstract

Objective

This study aimed to investigate the effects of Chitosan/Alginate-loaded *Astragalus hamosus* extract (AH) on the expression of miRNA-222 and ESR1 genes, pro-inflammatory cytokines, lipid profiles, and sex hormone levels in rats with PCOS-induced by estradiol valerate (EV).

Methods

25 female Wistar rats, with an average weight of 180 g, were divided into control and PCOS groups. The PCOS model was induced by a single intramuscular injection of EV (4 mg/kg). After 28 days of PCOS induction, the rats were orally administered Chitosan/Alginate-loaded AH at doses of 5, 10, and 15 mg/kg. Following four weeks of treatment, histological and biochemical parameters, pro-inflammatory cytokines, body weight, and the expression of miRNA-222 and ESR1 genes were evaluated.

Results

EV-induced PCOS rats exhibited a significant increase in body weight, abnormal lipid profiles, elevated pro-inflammatory cytokine levels, altered sex hormone levels, upregulation of miRNA-222 expression, and downregulation of ESR1 gene expression. The administration of Chitosan/Alginate-loaded AH (Chn/Al-AH) demonstrated ameliorative effects on the PCOS rats, restoring both endocrine and metabolic abnormalities to normal levels and attenuating complications in EV-induced PCOS rats. Notably, it significantly reduced miRNA-222 expression and promoted follicular development at various stages while reducing cystic follicles and increasing corpus luteum formation.

Conclusions

Chn/Al-AH was found to have beneficial effects in attenuating and improving certain complications in the PCOS rat models.

Introduction

Polycystic ovary syndrome (PCOS), also known as Stein-Leventhal syndrome, is a heterogeneous and multifactorial disorder and one of the main causes of infertility among women of reproductive age [1, 2]. Classical features of PCOS include systemic metabolic impairment, hormonal imbalances in reproduction, anovulation, and polycystic ovaries [3]. It is closely related to the hypersecretion of LH, which is the most common manifestation of PCOS, hyperandrogenism, and dyslipidemia [4, 5]. A higher LH/FSH ratio leads to increased levels of testosterone and estrogen, ultimately resulting in the formation

of a large number of follicles [6]. An increase in systemic serum pro-inflammatory mediators, including IL-18, TNF-α, and IL-6, appears to be both a cause and an effect of the syndrome [7, 8].

Several studies have reported a significantly different expression profile of miRNAs in patients with PCOS [9, 10]. For example, some studies have shown the overexpression of miR-21, miR-27-b, miR-103, miR-155, and miR-222 [11, 12], while others have found lower expression of miR-6767-5p in women with PCOS [13].

Conventional pharmacological therapy is limited due to the prevalence of contraindications and unwanted side effects. Herbal medications exhibit an alternative therapy for managing and ameliorating metabolic disorders, including PCOS [14, 15]. *Astragalus hamosus* (AH) is one of the most important herbs with a broad range of traditional treatments. It is an annual plant with a height of 20-30cm. Strongly curved fruits are the feature of this plant. AH has been used to treat diverse diseases in the Middle East and Persian traditional medicine [16]. The anti-inflammatory effects of AH have also been demonstrated [17]. In Iranian traditional and folk medicine, AH is recommended for the regulation of the estrous cycle by herbalists. Chitosan (Chn) is widely utilized as a delivery matrix for controlled drug release in both animals and humans [18]. It shows nontoxicity, biodegradability, and immunomodulatory activities, making it highly attractive for various biomedical applications [19]. However, chitosan's limited solubility, which is enhanced in acidic aqueous solutions, and its dominant structure, composed of 2-amino-2-deoxy-D-glucopyranose units, pose challenges and restrict potential applications. To overcome this limitation, modifying the structure of chitosan by incorporating hydrophilic functional groups, such as alginate (Al) has been employed to enhance its solubility [20].

As there is no existing evidence indicating the effects of Chitosan/Alginate hydrogel-loaded AH extract (Chn/Al-AH) on PCOS, we hypothesized that Chn/Al-AH might have beneficial effects in ameliorating PCOS complications. To test this hypothesis, our study aimed to examine the effects of different concentrations of Chn/Al-AH on serum reproductive hormone levels, lipid profiles, and pro-inflammatory markers. In addition to these biochemical biomarkers, we also investigated miR-222 and ESR1 gene expression as well as the number of follicles using an experimental PCOS model.

Materials & methods

Plant collection, authentication, and extraction

The fruits of AH were purchased from Tabriz (East Azerbaijan, Iran). These experiments received approval from the National Medicinal Plant Research Center of Shahid Beheshti University of Medical Sciences. The AH species was identified and authenticated by Dr. Samad Ebrahimi, a botanist at the Faculty of Medicinal Plants and Drugs Research, Shahid Beheshti University, Tehran, Iran. A voucher specimen (333HMS) [21] was deposited in the herbarium of the Faculty of Medicinal Plants.

Approximately 80–120 fruits from fresh plants were dried at room temperature to obtain 100 mg of the extract. The dried fruits were then powdered and subjected to Soxhlet extraction with absolute ethanol.

Specifically, 100 g of AH powder was extracted with 400 ml of absolute ethanol for 8 hours. The solution was filtered and evaporated to half its volume at 40°C. Subsequently, the extracts were concentrated and filtered using a 0.22 µm membrane PVDF syringe filter and stored at 4°C. GC–MS analysis of the extract has been reported in our previous study [22].

Dose selection and levels of the extract

To prepare chitosan coatings, 10 ml of alcoholic extract was used which contained 2.5 g of dry extract. Three doses of chitosan coatings were selected to evaluate the effectiveness of the extract, which consisted of 5, 10, and 15 ml of extract coated on dried chitosan. These doses were equivalent to approximately 1.25, 2.5, and 3.75 mg of dry AH extract.

Fabrication of chitosan/alginate hydrogel and loading of AH extract (Chn/Al-AH)

Commercial chitosan (Flonac C) was purchased from Nippon Suisan Kaisha, Japan, and sodium alginate was obtained from Sigma. Chitosan was dissolved overnight in 0.1M acetic acid under stirring at room temperature, and the pH of the solution was adjusted to 6.5. Subsequently, 10 ml of AH extract was added to this solution. The modification of chitosan was also carried out using an aqueous solution of sodium alginate. For this purpose, 0.5 g of sodium alginate was dissolved in 50 ml of deionized water, and the pH of the solution was adjusted to 6.5. Aqueous calcium chloride solution was added drop by drop to 10 ml of sodium alginate and stirred for one hour. Then it was added to the chitosan solution and stirred vigorously. Subsequently, 10 ml of AH extract was added to this solution. The prepared solution was then added drop by drop to 100 ml of an aqueous solution containing 2 g of sodium tripolyphosphate (STPP) and 1.5 g of sodium hydroxide. Finally, the prepared hydrogels were left at room temperature for 24 hours and then dried at 40°C.

Analysis of Fourier Transforms Infra-Red spectroscopy (FTIR)

Fourier transforms infrared spectra were obtained using a PerkinElmer FT-IR Spectrophotometer to detect the functional groups involved in the hydrogel synthesis.

Field Emission Scanning Electron Microscopy and Energy Dispersive X-ray Spectroscopy

The surface morphology of Chn/Al-AH was investigated using Field Emission Scanning Electron microscopy (FE SEM) (Sigma VP, ZEISS, Germany; equipped with EDS and Mapping detectors from Oxford Instruments, UK). The SEM apparatus was equipped with an EDAX PV7715/89-ME energy dispersive X-ray (EDX) spectrometer.

Animal experiments

In this study, 25 adult Wistar female rats (Rattus norvegicus), aged 7–8 weeks and weighing 180 ± 5 g, were purchased from the Animal Research Center (Tabriz University, Tabriz, Iran). All rats were housed in standard polypropylene cages, maintained at a controlled room temperature of 25°C, with a 12-hour light and 12-hour dark cycle in a well-ventilated room for two weeks. During the adaptation period, they had free access to food and water. All the experimental protocols were approved by the Animal Care and Ethics Committee of Islamic Azad University, Urmia branch, Urmia, Iran (IR.IAU.URMIA.REC.1398.023).

PCOS induction

After acclimatization, the rats were randomly divided into two experimental groups: the control group (n = 5) and the PCOS group (n = 20), once they had completed 2–3 estrus cycles, which typically took 12–14 days. PCOS was induced by a single intramuscular injection of Estradiol Valerate (EV) at a dose of 4 mg/kg body weight of the rats (Aburaihan Pharmaceutical Co., Tehran, Iran) [23]. The rats were housed in special cages for eight weeks and provided with a daily diet of 20 mg/day of commercially available regular pellets and water. The successful induction of the syndrome over eight weeks was monitored using the pipette smear technique, which involves assessing the ratio of cornified cells to epithelial cells.

Vaginal smear cytology

The pipette smear technique was performed daily to collect smear samples from the rats' vaginas, typically between 8:30 AM and 9:00 AM, and this continued until the last day of the study. A sterile cotton swab was soaked in 0.9% saline before being gently inserted into the animals' vaginas. While carefully holding the tail in one hand, the swab was gently rotated around the first 1/3 of the vaginal wall. Cells from the vaginal lumen and walls were gently removed and smeared in the same direction on a clean, grease-free microscope slide, and then air-dried. The air-dried smears were fixed in absolute ethanol, stained with Giemsa (diluted 1:10 v/v), and analyzed using a light microscope at a 10x objective lens.

Animal grouping

PCOS rats were divided into five experimental groups and were treated for four weeks; including:

- Normal healthy animals (n = 5): Control;
- EV (n = 5): PCOS;
- Three experimental groups including PCOS rats received three different doses of Chn/Al-AH including 5, 10, and 15mg/kg/day (n = 5 for each group):

PCOS + 5mg Chn/Al-AH;

PCOS + 10mg Chn/Al-AH;

PCOS + 15mg Chn/Al-AH.

Collection of blood samples and serum biochemical analysis

After 28 days of continuous treatment, the rats were anesthetized using an intraperitoneal injection of a ketamine/xylazine cocktail (Ketamine 60 mg/kg, Xylazine 20 mg/kg) after fasting overnight for 12 h. Following anesthesia, blood samples were collected from the abdominal aorta into plain EDTA red-top tubes. Blood continued to flow into dry tubes until the animals passed away. To obtain serum, the samples were allowed to clot for 2 h at room temperature before centrifugation. The tubes were then centrifuged at 3000 rpm for 15 min in a refrigerated centrifuge, and the serum was extracted. The serum concentrations of progesterone, estrogen, follicle-stimulating hormone (FSH), luteinizing hormone (LH), and testosterone were determined using enzyme-linked immunosorbent assay (ELISA) kits specific to each parameter (Cusabio Biotech Co., China). The serum lipid profile including high-density lipoprotein (HDL) cholesterol, low-density lipoprotein (LDL) cholesterol, triglyceride (TG), total cholesterol (TC), and very-low-density lipoprotein (VLDL) was assayed using standard ELISA kits (Pars Azmoon Inc., Tehran, Iran). The concentrations of IL-6, IL-18, and TNF-α were determined using ELISA-specific kits (Fine Test Co. China).

Histopathological studies and follicle count

Rats were sacrificed by cutting off the diaphragm, after which the ovaries were identified and dissected from the surrounding fat. The right ovaries and uterine tissues were placed in 10% formalin, dehydrated with graded ethanol, cleared with xylol, and finally embedded in paraffin. Histological sections were prepared using a rotary microtome at a thickness of 5 µm and stained with Hematoxylin and Eosin (H&E) dye. Morphometric analysis of uterine, ovaries, and follicle counting was performed using a light microscope. The total numbers of primary, pre-antral, antral, cystic, and corpus luteum follicles were counted. Animal body weights were recorded weekly from day 0 until the end of the study. The uterus and left ovarian tissue samples were kept at − 80°C for molecular evaluation.

RNA extraction and Quantitative reverse transcription (qRT-PCR)

Total RNA was extracted from the uterus and ovarian tissues using an RNX-plusTM kit (Gene All, Korea) according to the manufacturer's protocol. The quality and concentration of RNA were determined using a spectrophotometer by measuring absorbance at 260 and 280 nm. For complementary DNA (cDNA) synthesis, six micrograms and 50 ng of the total RNA were transcribed using a Zistroyesh microRNA detection kit, Tehran, Iran, and Royan Biotech kit, Tehran, Iran for miRNA-222 and ESR-1 respectively. Quantitative reverse transcription-PCR (qRT-PCR) was performed in duplicate, using 10 µl SYBR Green qPCR Master Mix (2X) (Pishgam. Tehran, Iran), 8 pm from each forward and reverse primers and 2µl of cDNA for each reaction in a final volume of 20µl. Primer sequences of miRNA-222 and U6 were prepared using the Zistroyesh microRNA detection kit (Zistrooyesh, Tehran, Iran). miRNA-222 and its target gene, *ESR1*were normalized by the reference genes, U6 and ACTIN, respectively, and calibrated for each sample against the control. Primers for rat ACTIN (Forward: 5'- CTCATGAAGATCCTGACCGAG − 3', Reverse: 5'- TCTCTTTAATGTCACGCACGA − 3') and ESR1 (Forward: 5'-TTGATCACACACCGCGCCACT-3', Reverse: 5'- CCCTGCTGGTTCAAAAGCGTCT-3') were designed using NCBI website. The relative intensity of expression was calculated by the $2^{-\Delta\Delta Ct}$ method.

Statistical analysis

All data were expressed as mean ± standard error (SEM). The statistical analysis of the experiments was conducted using SPSS v 22.0 and GraphPad Prism version 7 software. One-way ANOVA, followed by Duncan's multiple post hoc test, was used to compare the mean differences of the multiple samples. Differences were considered significant at $P < 0.05$.

Results

Characterization of chitosan hydrogel and loaded extract by FTIR and SEM analysis

The significant peaks were observed in three regions at 3200–3500 cm^{-1}, associated with the NH_2, O–H stretch, and C-H functional groups. These peaks indicate the absorption of water and moisture onto the hydrogel. The peaks in the range of 1652 – 1595 cm^{-1} are attributed to the amide groups of chitosan and alginate. The recorded results also reveal distinctive spectral patterns at 1000–1250 cm^{-1}, which are attributed to STPP. Furthermore, a new peak appeared at 1431 cm^{-1}, indicating the conjugation of chitosan and alginate. The absorption band at 1637 cm^{-1} originated from the electrostatic interaction between the -COOH groups of alginic acid and the -NH_2 groups of chitosan (Fig. 1A).

FESEM images in Fig. 1B depict the shape, size, and morphology of the hydrogel matrix. These images reveal the interior structures of the dried hydrogels related to chitosan (Fig. 1B, a), chitosan/alginate (Fig. 1B,b), and Chn/Al-AH (Fig. 1B,c), respectively. In all cases, the hydrogels exhibit a porous three-dimensional structure, resulting from phase separation and the evaporation of water during drying. Numerous wrinkles and several cavities are visible on the surface of the pure hydrogels due to incomplete network collapses during drying. Moreover, the surface of the microparticles is not smooth but displays bumps and pores, which effectively encapsulate the extract and facilitate its diffusion.

Analysis of the elements in a gold-covered specimen and dot mapping of chitosan/alginate, as shown in the EDX pattern, confirms the presence of C and O elements while revealing the absence of any extraneous elements, thereby confirming the purity of these particles. Notably, the observed peak at 1.2 ekV corresponds to the presence of gold. Based on the results, the highest percentage is attributed to the C element, indicating the significant contribution of chitosan and alginate (Fig. 1C). The dot mapping also shows the uniform distribution of elements on the surface of hydrogels (Fig. 1D).

Estrous cycle

Evaluation of estrous cyclicity in rats was determined based on the presence/absence and proportion of epithelial cells, cornified cells, and leukocytes [24]: The Proestrus stage (the first stage) with the presence of small and oval nucleated epithelial cells. The Estrous stage (the second stage) is mainly with the presence of extensive cornified keratinocytes with irregular shapes. The Metestrus (the third

stage) is by nucleated epithelial keratinocytes and a few leukocytes. The Diestrus stage (the fourth stage) by high numbers of leukocytes and fewer nucleated epithelial cells. EV-induced PCOS rats showed an irregular estrous cycle (Fig. 2).

Assessment of bodyweight

Body weight showed a significant increase (P 0.001) in PCOS rats when compared with the control group. Treatment with 10 and 15mg of Chn/Al-AH showed a significant decrease (P 0.001) in body weight compared to the PCOS group (Table 1).

Table 1 Comparative assessment of the body weight between the control, PCOS, and experimental groups.

Groups	Body Weight (g)	P Value compared to the PCOS group
Control	180 ± 10g	***P<0.0001
PCOS	230 ± 10g	
PCOS-5mg Chn/Al-AH	205 ± 10g	**P<0.001
PCOS-10mg Chn/Al-AH	190 ± 10g	***P<0.0001
PCOS-15mg Chn/Al-AH	180 ± 10g	***P<0.0001

Ovarian Histomorphology

Healthy follicles with normal morphologies at different stages of development were observed in the control group. In contrast, an increase in cystic follicles and a decrease in follicular clusters and corpus luteum were seen in the PCOS group. The number of corpus luteum increased in the treatment groups compared to the PCOS group. Furthermore, the number of corpus luteum was greater in the PCOS + 15mg Chn/Al-AH group than in the other treatment groups (Fig. 3).

The number of primary follicles showed no significant difference in the studied groups. In contrast, the number of pre-antral and antral follicles, as well as corpus luteum, significantly decreased in the PCOS group compared to the control group ($P < 0.01$ and $P < 0.001$). Treatment with 10 and 15mg of Chn/Al-AH resulted in a significant increase in pre-antral, antral follicles, and corpus luteum compared to the PCOS group ($P < 0.05$, $P < 0.01$, and $P < 0.001$), accompanied by a significant decrease in the number of cystic

follicles ($P < 0.01$). The CL/CF ratio showed a significant increase with 10 and 15mg of Chn/Al-AH, compared to the PCOS group ($P < 0.001$) (Fig. 4).

Uterine Histomorphology

The conventional morphological measurement method was used for histomorphometric analysis. For this, H&E uterine sections of all groups were visualized using a light microscope. Figure 5 illustrates the uterine photomicrographs from all experimental groups. Normal thickened endometrium with a single and straight layer of columnar epithelium without any convolution (Fig. 5A), neat arrangement of the nuclei without consolidation (Fig. 5A1), and single tubular uterine glands (Fig. 5A2) were observed in the control group. In contrast, endometrial hyperplasia was detected in the PCOS group (Fig. 5B). In the luminal epithelium hyperplasia, a profound increase in the epithelial cells height and thickening was identified by the formation of multiple poor columnar and pseudostratified epithelium and due to the rapid proliferation of the epithelial cells (Fig. 5B1). Histological analysis also showed glandular hyperplasia, including irregular folds of the endometrium toward the uterine lumen, cystic dilatation, and convolution of endometrial glands (Fig. 5B2). Furthermore, the invagination of the thickened epithelium in the underlying stroma formed ciliated-shaped cells in the stroma (Fig. 5B3). The number of endometrial glands decreased compared to the control group. In addition, some conglomerate (Fig. 5B4) and cystic glands (Fig. 5B5) were observed in the field of view (Fig. 5). Relative resuming of normal histological structures of the uterine were observed in the treatment groups (Fig. 5C). Treatment with 10 and 15mg of Chn/Al-AH showed mild and relatively improved endometrial hyperplasia, demonstrated by short endometrial folds toward the uterine lumen. Furthermore, a decrease in the thickness and the height of epithelial cell layers and an increase in the number of endometrial glands were observed after treatment compared to the PCOS group (Fig. 5C1-5).

Serum sex hormone level

As represented in Fig. 6, Serum FSH levels showed a significant decrease ($P < 0.001$) in the PCOS group when compared to the control group. Serum LH level and LH/FSH ratio were significantly increased in the PCOS group in comparison to the control group ($P < 0.01$ and $P < 0.001$ respectively). LH and FSH levels were not altered significantly after treatment in comparison to PCOS. LH/FSH ratio in the PCOS group was significantly reduced by all treatment groups ($P < 0.05$ and $P < 0.01$). Significant increases in testosterone and estrogen levels along with a significant decrease in progesterone levels were observed in the PCOS group when compared to the control group ($P < 0.001$). Applying Chn/Al-AH at all doses significantly decreased testosterone and estrogen compared to the PCOS group ($P < 0.01$ and $P < 0.001$ respectively), whereas progesterone levels showed a significant increase when compared with the PCOS group ($P < 0.001$).

Serum lipid profile

Figure 7 shows that the PCOS group had significantly higher levels of TG, TC, LDL, and VLDL ($P < 0.01$ and $P < 0.001$) and significantly lower levels of HDL ($P < 0.001$) than the control group. AH significantly

reduced blood levels of these markers ($P < 0.05$, $P < 0.01$, and $P < 0.001$) and significantly increased HDL levels ($P < 0.001$). However, a significant reduction in TG levels was observed only at 15mg of Chn/Al-AH ($P < 0.05$).

Serum inflammatory markers

All of the inflammatory markers were significantly increased in the PCOS group compared to the control group ($P < 0.01$ and $P < 0.001$), as shown in Fig. 8. Significant decrease in TNF-α and IL-6 levels was observed in 10 mg and 15 mg of Chn/Al-AH treatments when compared to the PCOS group ($P < 0.05$ and $P < 0.01$ respectively). None of the treatment groups showed a significant decrease in IL-18 levels when compared to the PCOS group.

mRNA expression of miRNA-222 and ESR1

Significant upregulation ($P < 0.001$) of miRNA-222 was observed in the PCOS group compared to the control group. This high expression was significantly reduced ($P < 0.01$, $P < 0.001$) through treatment with 5mg, 10mg, and 15mg of Chn/Al-AH. There was no significant difference in *ESR1* expression between the PCOS and control groups. Furthermore, applying 5mg and 10 mg of the Chn/Al-AH did not result in a significant increase in ESR1 expression compared to the PCOS group. However, a significant increase ($P < 0.05$) was observed only in the 15 mg treatment group compared to the PCOS group (Fig. 9).

Discussion

In the present study, the ameliorative effects of Chn/Al-AH in EV-induced POCS rats were investigated for the first time. To induce the PCOS model in rats, Estrogen and drugs with estrogenic effects are commonly used, as these compounds prompt morphological effects similar to those seen in PCOS [25]. Similar to the findings of Farhadi-Azar et al. [26], Our study indicated that EV is efficient enough to induce PCOS in rats.

Furthermore, this study revealed a greater weight gain in the PCOS group than in the control group, which is consistent with earlier studies [27]. However, all treated animals with Chn/Al-AH showed reduced body weight. Ovarian biopsy and biochemical parameters are commonly used for PCOS diagnosis. In this study, we considered both histological and biochemical evaluations. Abnormal changes in sex hormone levels, such as elevated estrogen, testosterone, and LH, and decreased FSH and progesterone levels, are major diagnostic criteria for PCOS [28]. In our study, the induction of PCOS significantly increased serum levels of estrogen and testosterone while decreasing serum progesterone levels. These findings are consistent with previous studies [27, 29]. A significant decrease in estrogen levels was observed after treatment with Chn/Al-AH. In parallel, the administration of Chn/Al-AH significantly increased progesterone levels in the treatment groups. These results are in line with previous studies [27, 29]. Furthermore, we observed a significant decrease in serum testosterone levels after treatment with all doses of Chn/Al-AH, which aligns with previous studies [29, 30]. We did not observe significant changes in LH and FSH levels in the groups receiving Chn/Al-AH compared to the PCOS group.

An increased LH-to-FSH ratio is a characteristic of PCOS [31]. In our study, the LH/FSH ratio in the PCOS group was statistically higher than in the control group. Chn/Al-AH significantly reduced the LH/FSH ratio in the treatment groups when compared to the PCOS group. These results are consistent with the previous studies [30, 32].

Histomorphologically, the presence of cystic follicles along with the absence of corpus luteum represent an indicator of ovarian dysfunction and anovulation. It could be correlated with an unusual rise in serum levels of androgens, indicating PCOS [33]. Subsequently, it causes to decrease or lack of progesterone which leads to endometrial overgrowth and hyperplasia [34].

Focusing on our results, EV-induced PCOS showed an increased number of cystic follicles, absence/or very few corpus luteum along with fewer antral or Graffian follicles [35, 36], which is considered as the cessation of folliculogenesis. Chn/Al-AH increased corpus luteum and follicles at different stages of development and decreased cystic follicles, indicating the recovery of the normal histology and finally ovulation in PCOS rats, aligned with the results of previous studies [36–39]. According to the findings of this study, Chn/Al-AH at 10 mg and 15 mg doses had better-normalizing effects on ovarian morphology.

The presence of endometrial hyperplasia in the uteri is considered a histological indicator of PCOS [40]. Our results indicated that abnormal alteration of uterine morphology including hyperplasia, decreased number of endometrial glands, the appearance of cystic glands, and thickening of the lining epithelium were obvious in the PCOS group consistent with previous studies [41, 42]. In this study, two types of endometrial glands were detected in the uterine sections according to Gunin et al. [43] including normal and cystic glands. Photomicrographs of the control group showed normal endometrial glands represented as simple tubular glands with an oval, round, or elongated shape and narrow lumen. In the PCOS group, cystic glands with a large size and round shape were observed.

Treatment with 10 and 15mg of Chn/Al-AH revealed the relative resuming of normal uterine structure. The epithelium thickness decreased and the number of normal endometrial glands increased after treatment. These findings agree with the results of previous studies, in which various treatments including Silibinin [42], Melatonin and Metformin [44], Vitamin D [45], Metformin [41], dodder total flavone [46], and *Ageratum conyzoides* [36] were used.

The study by Adelakun et al. demonstrated a correlation between higher levels of TG, TC, and LDL on one hand, and lower levels of HDL on the other hand, with anovulation in PCOS [36]. The findings of this study revealed a significant increase in serum concentrations of TC, LDL, TG, and VLDL, along with a significant decrease in HDL levels in the EV-induced PCOS rats. Treatment with 10 mg and 15 mg doses of Chn/Al-AH significantly reversed the abnormal lipid profiles observed in the PCOS group. These results are consistent with previous findings, such as those from studies using Sumac [47], Genistein for LDL [37], Polyherbal syrup [29], Ginger [48], *Ageratum conyzoides* [36], and *Agaricus subrufescens* for TG and TC [49].

Given the crucial role of pro-inflammatory factors in determining the inflammatory state in PCOS, this study assessed serum levels of TNF-α, IL-6, and IL-18. Previous studies have reported elevated levels of TNF-α and IL-6 in PCOS [36, 50]. Several studies have shown significant reductions in the levels of these factors after treatment with compounds such as Gallic Acid [51], hawthorn leaf flavonoids [52], Quercetin [53], resveratrol for TNF-α [32], saffron [54], and *Ageratum conyzoides* [36].

In the present study, increased levels of TNF-α, IL-6, and IL-18 were observed in the PCOS group, likely attributed to the effectiveness of EV in inducing PCOS in rats. Chn/Al-AH-treated groups at doses of 10 mg and 15 mg demonstrated a significant reduction in TNF-α and IL-6 levels when compared to the PCOS group. These findings are consistent with the previously mentioned studies. However, it is noteworthy that our results regarding IL-18 did not exhibit significant changes after treatment with the Chn/Al-AH.

It has been demonstrated that increased miR-222 expression is linked to PCOS and may play a significant role in the development of this condition [55].

The results obtained from this study showed a noteworthy increase in miRNA-222 expression in the PCOS group when compared to the control group, consistent with the earlier studies [12].

A significant decrease in miR-222 expression was observed after treatment with all doses of the Chn/Al-AH in comparison to the PCOS group. These outcomes concur with the findings of Huang et al. and Almalki et al., in which the expression levels of miRNA-222 exhibited significant decreases following treatment [12, 56]. It has been well-documented that the upregulation of miRNA-222 in PCOS negatively regulates estrogen receptor alpha [57]. Gianpiero Di Leva et al. reported a reciprocal negative regulatory loop between miRNA-222 and the ESR1 gene, wherein miRNA-222 represses ESR1[58].

In this study, neither the control group nor the treatment groups displayed significant differences in the expression of ESR1 when compared to the PCOS group. It may be due to that miRNA-222 might indirectly facilitate ESR1/estrogen signaling by directly inhibiting BECLIN1. The interaction between ESR1 and BECLIN1 could potentially influence the functions of both BECLIN1 and ESR1 as downstream targets of miRNA-222. It is conceivable that a reciprocal regulatory mechanism between BECLIN1 and ESR1 might yield unfavorable outcomes, including the negative modulation of ESR1 [59]. Furthermore, endometrial hyperplasia seems to be dependent on ESR1 activation [60]. Our treatments were not successful enough to completely improve the uterine tissue changes and resume the normal uterine tissue architecture including the absence of hyperplasia. It may be due to the insufficient time duration of our treatment. This area remains an important subject for future investigations to address the effect of long-term treatment with Chn/Al-AH on endometrial hyperplasia and its relation with the expression of ESR1.

Given the widespread and unbridled use of natural herbs and edible products by the general population, it has become necessary to assess their safety on body functions including the female reproductive system. For the first time, the findings of this study indicate that Chn/Al-AH improves the ovary function

impairments in the PCOS, as evidenced by a significant decrease in cystic follicles, LH/FSH ratio, serum levels of TNF-α, IL-6, triglyceride, cholesterol, LDL, estrogen, and testosterone and *miRNA-222* expression and also a significant increase in corpus luteum, serum levels of progesterone, HDL, and ESR1 expression (Fig. 9). In summary, Chn/Al-AH can achieve a balance in histological, hormonal, lipid profile, inflammatory and genetic aspect of PCOS.

However, it is important to note that this study has its limitations. There was no group treated with a routine drug commonly used to treat PCOS, such as metformin. Including such a group in future studies would allow for a direct comparison between the effects of Chn/Al-AH and conventional treatments.

Conclusion

In this study, Chn/Al-AH hydrogels were successfully synthesized, and physicochemical properties confirmed their properties. The present study provided an initial insight into the potential ameliorating effects of Chn/Al-AH on the female reproductive system. The consumption of Chn/Al-AH was found to result in an increase in corpus luteum and a decrease in cystic follicles. Serum sex hormone level, inflammatory markers, and lipid profile were also balanced after treatment with Chn/Al-AH. The results of this study suggest that Chn/Al-AH could be an effective component in addressing a wide range of complications associated with PCOS. Further research is required to delineate the detailed underlying molecular mechanisms of Chn/Al-AH that ameliorate the symptoms of PCOS.

Abbreviations

PCOS: Polycystic ovary syndrome; qRT-PCR: Quantitative reverse transcription- PCR; ELISA: Enzyme-linked immunosorbent assay; STPP: Sodium triphosphate; PVC: Persistent vaginal cornification; cDNA: Complementary DNA; FTIR: Fourier-transform infrared spectroscopy; CF: Cystic follicles; CL: Corpus luteum; ESR1: Estrogen receptor 1; EDX: Energy dispersive X-Ray Spectroscopy; FOSL1: FOS-like antigen 1; FSH: Follicle stimulating hormone; LH: Luteinizing hormone; HDL: High-density lipoprotein; LDL: Low-density lipoprotein; TG: Triglyceride; TC: Total cholesterol: VLDL: Very-low-density lipoprotein: IL-6: Interleukin-6; TNF-α: Tumor necrosis factor-α; AH: *Astragalus hamosus*; Chn/Al-AH: Chitosan/alginate hydrogel-AH; EV: Estradiol valerate.

Declarations

Acknowledgments

In the name of Allah. We express our appreciation to Dr. Hossein Ghanbarian and Dr. Farhad Farhanpajouh for their technical and scientific assistance.

Authors' contributions

M. Parvini Kohnehshahri conceived and designed the project. R. Jafardoust Bostani and A. Pouryaee performed experiments under the supervision of M. Parvini Kohnehshahri. Z. Ghazi Tabatabaei and M. Parvini Kohnehshahri supervised overall data generation and analysis. M. Parvini Kohnehshahri wrote the manuscript with the help of other authors. All authors contributed to the article, approved the final manuscript, and have no competing interests.

Funding

This research did not receive any specific grant from funding agencies in the public, commercial, or not-for-profit sectors.

Availability of data and materials

The data that support the findings of this study are available from the corresponding author, Dr. Maryam Parvini Kohnehshahri, upon reasonable request.

Ethics approval and consent to participate

The research protocols used in this research were approved by the Ethical Committee of the Islamic Azad University, Urmia Branch, Iran (IR.IAU.URMIA.REC.1398.023). Animal care or treatments were in agreement with the Animal Care and Use Protocol of Islamic Azad University, Urmia Branch, Iran

Consent for publication

Not applicable.

Competing interests

The authors declare no conflict of interest.

Author Details

[1]Department of Biology, Urmia Branch, Islamic Azad University, Urmia, Iran

[2]Department of Chemistry, Ahar Branch, Islamic Azad University, Ahar, Iran

References

1. Azziz R, Woods KS, Reyna R, Key TJ, Knochenhauer ES, Yildiz BO. The prevalence and features of polycystic ovary syndrome in an unselected population. J Clin Endocrinol Metab. 2004;89(6):2745–49.
2. Azziz R, Adashi EY. Stein and Leventhal: 80 years on. Am J Obstet Gynecol. 2016;214(2):247. e1-247.e11.

3. Di Lorenzo M, Cacciapuoti N, Lonardo MS, Nasti G, Gautiero C, Belfiore A, Guida B, Chiurazzi M. Pathophysiology and Nutritional Approaches in Polycystic Ovary Syndrome (PCOS): A Comprehensive Review. Curr Nutr Rep. 2023;12(3):527–44.
4. Guo F, Gong Z, Fernando T, Zhang L, Zhu X, Shi Y. The Lipid Profiles in Different Characteristics of Women with PCOS and the Interaction Between Dyslipidemia and Metabolic Disorder States: A Retrospective Study in Chinese Population. Front Endocrinol (Lausanne). 2022;13:892125.
5. Chappell NR, Gibbons WE, Blesson CS. Pathology of hyperandrogenemia in the oocyte of polycystic ovary syndrome. Steroids. 2022;180:108989.
6. Xia Q, Xie L, Wu Q, Cong J, Ma H, Li J, Cai W, Wu X. Elevated baseline LH/FSH ratio is associated with poor ovulatory response but better clinical pregnancy and live birth in Chinese women with PCOS after ovulation induction. Heliyon. 2023;9(1):e13024.
7. Yang Y, Qiao J, Li R, Li MZ. Is interleukin-18 associated with polycystic ovary syndrome? Reprod Biol Endocrinol. 2011;9:7.
8. Zhai Y, Pang Y. Systemic and ovarian inflammation in women with polycystic ovary syndrome. J Reprod Immunol. 2022;151:103628.
9. Udesen PB, Sørensen AE, Svendsen R, Frisk NLS, Hess AL, Aziz M, Wissing MLM, Englund ALM, Dalgaard LT. Circulating miRNAs in Women with Polycystic Ovary Syndrome: A Longitudinal Cohort Study. Cells. 2023;12(7):983.
10. Sørensen AE, Wissing ML, Salö S, Englund AL, Dalgaard LT. MicroRNAs Related to Polycystic Ovary Syndrome (PCOS). Genes (Basel). 2014;5(3):684–708.
11. Murri M, Insenser M, Fernández-Durán E, San-Millán JL, Escobar-Morreale HF. Effects of polycystic ovary syndrome (PCOS), sex hormones, and obesity on circulating miRNA-21, miRNA-27b, miRNA-103, and miRNA-155 expression. J Clin Endocrinol Metab. 2013;98(11):E1835–44.
12. Huang X, She L, Luo X, Huang S, Wu J. MiR-222 promotes the progression of polycystic ovary syndrome by targeting p27 Kip1. Pathol Res Pract. 2019;215(5):918–23.
13. Huang CC, Yang PK, Huang YS, Chen SU, Yang YS, Chen MJ. The role of circulating miRNAs in mechanism of action and prediction of therapeutic responses of metformin in polycystic ovarian syndrome. Fertil Steril. 2023;119(5):858–68.
14. Lakshmi JN, Babu AN, Kiran SSM, Nori LP, Hassan N, Ashames A, Bhandare RR, Shaik AB. Herbs as a Source for the Treatment of Polycystic Ovarian Syndrome: A Systematic Review. BioTech (Basel). 2023;12(1):4.
15. Mihanfar A, Nouri M, Roshangar L, Khadem-Ansari MH, Polyphenols. Natural compounds with promising potential in treating polycystic ovary syndrome. Reprod Biol. 2021;21(2):100500.
16. Umer KH, Zeenat F, Ahmad W, Vakil K. Therapeutics, phytochemistry and pharmacology of Iklilul Malik (Astragalus hamosus Linn): A natural Unani Remedy. Int J Herbal Medicine. 2017;5(5):01–5.
17. Hakim A, Ghufran A, Nasreen J. Evaluation of anti-inflammatory activity of the pods of Iklil- ul-Malik (Astragalus hamosus Linn.). IJNPR. 2010; 1(1): 34–37. [18] V. Mikušová, P. Mikuš, Advances in Chitosan-Based Nanoparticles for Drug Delivery, Int J Mol Sci. 2021;22(17):9652.

18. Zhao D, Yu S, Sun B, Gao S, Guo S, Zhao K. Biomedical Applications of Chitosan and Its Derivative Nanoparticles. Polym (Basel). 2018;10(4):462.
19. Dai YN, Li P, Zhang JP, Wang AQ, Wei Q. Swelling characteristics and drug delivery properties of nifedipine-loaded pH sensitive alginate-chitosan hydrogel beads. J Biomed Mater Res B Appl Biomater. 2008;86(2):493–500.
20. Bahaeddin Z, Yans A, Khodagholi F, Sahranavard S. Neuroprotection and anxiety like behavior reduction of Allium hirtifolium and Astragalus hamosus in the Aβ-injected rat. RJP. 2016;3(4):39–49.
21. Nejati A, Parvini kohnehshahri M, Farahvash T. Astragalus hamosus Acts as an Insulin Sensitizer in the Treatment of Polycystic Ovary Syndrome Rat Models by Affecting IRS1 Expression. Endocr Metab Immune Disord Drug Targets. 2022;22(3):348–56.
22. Brawer JR, Munoz M, Farookhi R. Development of the polycystic ovarian condition (PCO) in the estradiol valerate-treated rat. Biol Reprod. 1986;35(3):647–55.
23. Cora MC, Kooistra L, Travlos G. Vaginal Cytology of the Laboratory Rat and Mouse: Review and Criteria for the Staging of the Estrous Cycle Using Stained Vaginal Smears. Toxicol Pathol. 2015;43(6):776–93.
24. Artini PG, Di Berardino OM, Simi G, Papini F, Ruggiero M, Monteleone P, Cela V. Best methods for identification and treatment of PCOS. Minerva Ginecol. 2010;62(1):33–48.
25. Farhadi-Azar M, Ghahremani M, Mahboobifard F, Noroozzadeh M, Yaghmaei P, Tehrani FR. Effects of Rosa damascena on reproductive improvement, metabolic parameters, liver function and insulin-like growth factor-1 gene expression in estradiol valerate induced polycystic ovarian syndrome in Wistar rats. Biomed J. 2023;46(3):100538.
26. Pournaderi PS, Yaghmaei P, Khodaei H, Noormohammadi Z, Hejazi SH. The effects of 6- Gingerol on reproductive improvement, liver functioning and Cyclooxygenase-2 gene expression in estradiol valerate - Induced polycystic ovary syndrome in Wistar rats. Biochem Biophys Res Commun. 2017;484(2):461–6.
27. Singh S, Pal N, Shubham S, Sarma DK, Verma V, Marotta F, Kumar M. Polycystic Ovary Syndrome: Etiology, Current Management, and Future Therapeutics. J Clin Med. 2023;12(4):1454.
28. Balasubramanian A, Pachiappan S, Mohan S, Adhikesavan H, Karuppasamy I, Ramalingam K. Therapeutic exploration of polyherbal formulation against letrozole induced PCOS rats: A mechanistic approach. Heliyon. 2023;9(5):e15488.
29. Gu M, Cai H, Deng W, Tang Y, Du S, Wang P, Deng W, Wang H, Sun A, Kong S. Dingkun pill alleviates metabolic abnormalities in polycystic ovary syndrome through brown adipose tissue activation. J Ovarian Res. 2023;16(1):176.
30. Malini NA, Roy K, George. Evaluation of different ranges of LH:FSH ratios in polycystic ovarian syndrome (PCOS) - Clinical based case control study. Gen Comp Endocrinol. 2018;260:51–7.
31. Furat Rencber S, Kurnaz Ozbek S, Eraldemır C, Sezer Z, Kum T, Ceylan S, Guzel E. Effect of resveratrol and metformin on ovarian reserve and ultrastructure in PCOS: an experimental study. J Ovarian Res. 2018;11(1):55.

32. Ndeingang EC, Defo Deeh PB, Watcho P, Kamanyi A. Phyllanthus muellerianus (Euphorbiaceae) Restores Ovarian Functions in Letrozole-Induced Polycystic Ovarian Syndrome in Rats. Evid Based Complement Alternat Med. 2019;2019:2965821.
33. Chandra V, Kim JJ, Benbrook DM, Dwivedi A, Rai R. Therapeutic options for management of endometrial hyperplasia. J Gynecol Oncol. 2016;27(1):e8.
34. Okafor IA, Nnamah US, Nnaka J. The fertility assessment of normal cyclic Wistar rats following the administration of methanolic extract of Portulaca oleracea: an experimental study. Middle East Fertil Soc J. 2021;26:5.
35. Adelakun SA, Ukwenya VO, Peter AB, Siyanbade AJ, Akinwumiju CO. Therapeutic effects of aqueous extract of bioactive active component of *Ageratum conyzoides* on the ovarian- uterine and hypophysis-gonadal axis in rat with polycystic ovary syndrome: Histomorphometric evaluation and biochemical assessment. Metabol Open. 2022;15:100201.
36. Amanat S, Ashkar F, Eftekhari MH, Tanideh N, Doaei S, Gholamalizadeh M, Koohpeyma F, Mokhtari M. The effect of genistein on insulin resistance, inflammatory factors, lipid profile, and histopathologic indices in rats with polycystic ovary syndrome. Clin Exp Reprod Med. 2021;48(3):236–44.
37. Namlı Kalem M, Anadol E, Kalem Z, Sezginer PY, Elmas C, Yılmaz C, Bakirarar B. A rat study on the PTEN expression in ovarian tissue in PCOS and folliculogenesis. Sci Rep. 2023;13(1):20774.
38. Falahatian S, Haddad R, Pakravan N. Modulatory effects of R10 fraction of garlic (Allium sativum L.) on hormonal levels, T cell polarization, and fertility-related genes in mice model of polycystic ovarian syndrome. J Ovarian Res. 2022;15(1):4.
39. Charalampakis V, Tahrani AA, Helmy A, Gupta JK, Singhal R. Polycystic ovary syndrome and endometrial hyperplasia: an overview of the role of bariatric surgery in female fertility. Eur J Obstet Gynecol Reprod Biol. 2016;207:220–6.
40. Zhang Y, Hu M, Meng F, Sun X, Xu H, Zhang J, Cui P, Morina N, Li X, Li W, Wu XK, Brännström M, Shao R, Billig H. Metformin Ameliorates Uterine Defects in a Rat Model of Polycystic Ovary Syndrome. EBioMedicine. 2017;18:157–70.
41. Marouf BH, Ismaeel DO, Hassan AH, Ali OJ. Therapeutic Effects of Silibinin Against Polycystic Ovary Syndrome Induced by Letrozole in Rats via Its Potential Anti-Inflammatory and Anti-Oxidant Activities. J Inflamm Res. 2022;15:5185–99.
42. Gunin AG, Mashin IN, Zakharov DA. Proliferation, mitosis orientation and morphogenetic changes in the uterus of mice following chronic treatment with both estrogen and glucocorticoid hormones. J Endocrinol. 2001;169(1):23–31.
43. Lohrasbi P, Karbalay-Doust S, Mohammad Bagher Tabei S, Azarpira N, Alaee S, Rafiee B, Bahmanpour S. The effects of melatonin and metformin on histological characteristics of the ovary and uterus in letrozole-induced polycystic ovarian syndrome mice: A stereological study. Int J Reprod Biomed. 2022;20(11):973–88.

44. Kuyucu Y, Çelik LS, Kendirlinan Ö, Tap Ö, Mete UÖ. Investigation of the uterine structural changes in the experimental model with polycystic ovary syndrome and effects of vitamin D treatment: An ultrastructural and immunohistochemical study. Reprod Biol. 2018;18(1):53–9.
45. Miao M, Peng M, Zhu Z, Yan X, Wei Z, Li M. Effects of dodder total flavone on polycystic ovary syndrome rat models induced by DHEA combined HCG. Saudi J Biol Sci. 2019;26(4):821–7.
46. Afandak F, Aryaeian N, Kashanian M, Janani L, Namizadeh T, Karimi MY, Morvaridi M. Effect of sumac powder on clinical symptoms, hyperandrogenism, inflammation, blood glucose, lipid profiles in women with polycystic ovary syndrome: A double-blind randomized clinical trial. Phytother Res. 2023;37(6):2315–25.
47. Tabibi H, Imani H, Atabak S, Najafi I, Hedayati M, Rahmani L. Effects of Ginger on Serum Lipids and Lipoproteins in Peritoneal Dialysis Patients: A Randomized Controlled Trial. Perit Dial Int. 2016;36(2):140–5.
48. Bukke SPN, Pathange BBR, Karumanchi SK, Marri J, Boyina R, Rachamsetty K, Manchikalapati B, Odoma S, Hussaini B. Agaricus Subrufescens ameliorates ovarian dysfunction and regulates altered biochemical parameters in rats with Letrozole induced polycystic ovarian syndrome. J Ovarian Res. 2023;16(1):221.
49. Wu G, Hu X, Ding J, Yang J. The effect of glutamine on Dehydroepiandrosterone-induced polycystic ovary syndrome rats. J Ovarian Res. 2020;13(1):57.
50. Mazloom BF, Edalatmanesh MA, Hosseini SE. Gallic acid reduces inflammatory cytokines and markers of oxidative damage in a rat model of estradiol-induced polycystic ovary. Comp Clin Pathol. 2019;28(5):1281–6.
51. Shi Y, Kong X, Yin H, Zhang W, Wang W. Effect of Hawthorn Leaf Flavonoids in Dehydroepiandrosterone-Induced Polycystic Ovary Syndrome in Rats. Pathobiology. 2019;86(2–3):102–10.
52. Vaez S, Parivr K, Amidi F, Rudbari NH, Moini A, Amini N. Quercetin and polycystic ovary syndrome; inflammation, hormonal parameters and pregnancy outcome: A randomized clinical trial. Am J Reprod Immunol. 2023;89(3):e13644.
53. Moshfegh F, Zafar Balanejad S, Shahrokhabady K, Attaranzadeh A. Investigating the Effect of Crocus sativus (Saffron) Petal Hydro-alcoholic Extract on Ovarian Follicle, Inflammatory Markers, and Antioxidant Enzymes in Mice Model of Polycystic Ovary Syndrome. J Reprod Infertil. 2022;23(1):18–25.
54. Soyman Z, Durmus S, Ates S, Simsek G, Sozer V, Kundaktepe BP, Kurtulus D, Gelisgen R, Sal V, Uzun H. CIRCULATING MIR-132, MIR-146A, MIR-222, AND MIR-320 EXPRESSION IN DIFFERENTIAL DIAGNOSIS OF WOMEN WITH POLYCYSTIC OVARY SYNDROME. Acta Endocrinol (Buchar). 2022;18(1):13–9.
55. Almalki WH, Alzahrani A, El-Daly M, Ahmed AF. A Critical Review of the Therapeutic Potential of Vitamin D-Mediated Suppression of miRNA222-Associated Metabolic Defects in Polycystic Ovarian Syndrome. Crit Rev Eukaryot Gene Expr. 2021;31(2):75–82.

56. Zhao JJ, Lin J, Yang H, Kong W, He L, Ma X, Coppola D, Cheng JQ. MicroRNA-221/222 negatively regulates estrogen receptor α and is associated with tamoxifen resistance in breast cancer. J Biol Chem. 2016;291(43):22859.
57. Di Leva G, Piovan C, Gasparini P, Ngankeu A, Taccioli C, Briskin D, Cheung DG, Bolon B, Anderlucci L, Alder H, Nuovo G, Li M, Iorio MV, Galasso M, Santhanam R, Marcucci G, Perrotti D, Powell KA, Bratasz A, Garofalo M, Nephew KP, Croce CM. Estrogen mediated- activation of miR-191/425 cluster modulates tumorigenicity of breast cancer cells depending on estrogen receptor status. PLoS Genet. 2013;9(3):e1003311.
58. John S, Nayvelt I, Hsu HC, Yang P, Liu W, Das GM, Thomas T, Thomas TJ. Regulation of estrogenic effects by beclin 1 in breast cancer cells. Cancer Res. 2008;68(19):7855–63.
59. Sá SI, Maia J, Bhowmick N, Silva SM, Silva A, Correia-da-Silva G, Fonseca N. BM.
60. Uterine histopathological changes induced by. acute administration of tamoxifen and its. modulation by sex steroid hormones. Toxicol Appl Pharmacol. 2019;363:88–97.

Figures

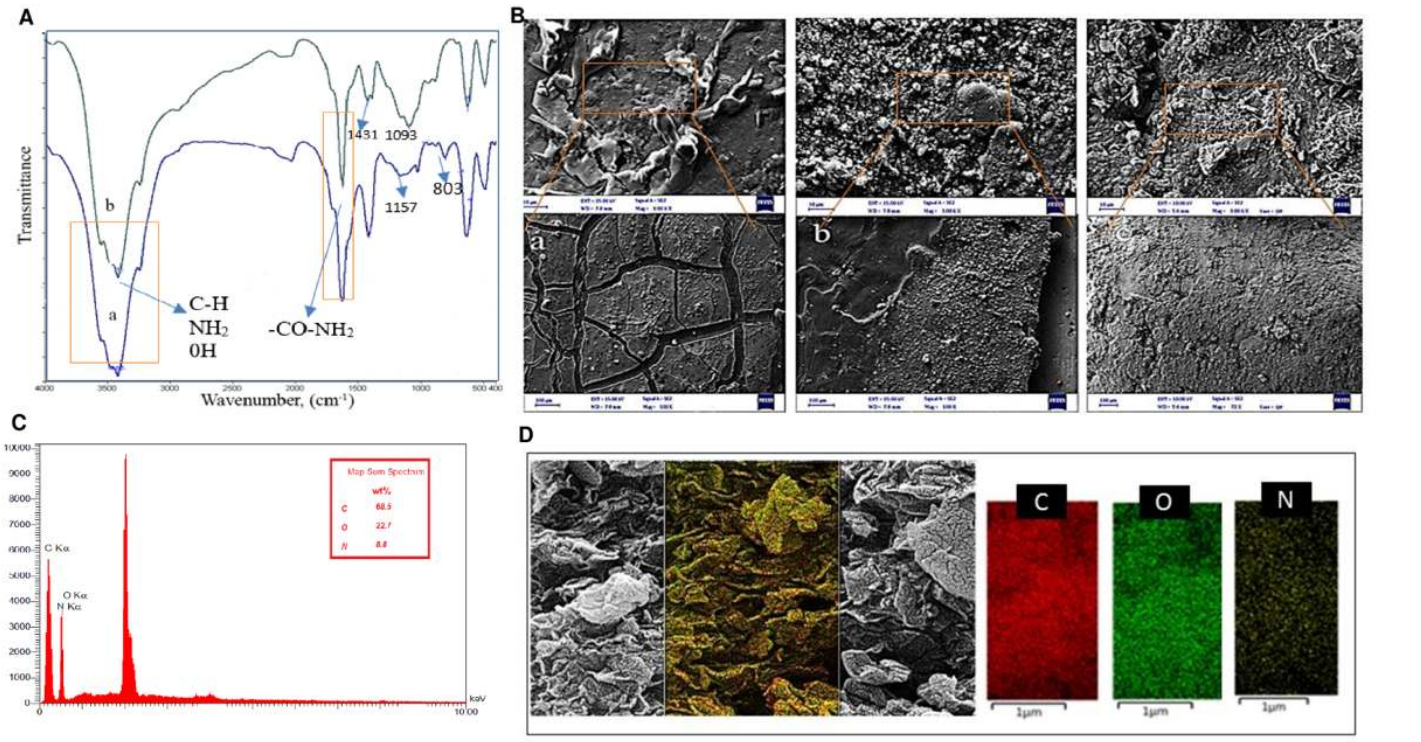

Figure 1

(**A**) FTIR spectrometry**,** chitosan/ alginate (**a**), chitosan/ alginate/extract (**b**); (**B**) FESEM photomicrographs of chitosan (**a**), chitosan/alginate (**b**), and chitosan/alginate-loaded AH extract (**c**); (**C**) and (**D**) Energy Dispersive Spectroscopy (EDX) and dot mapping of chitosan/alginate.

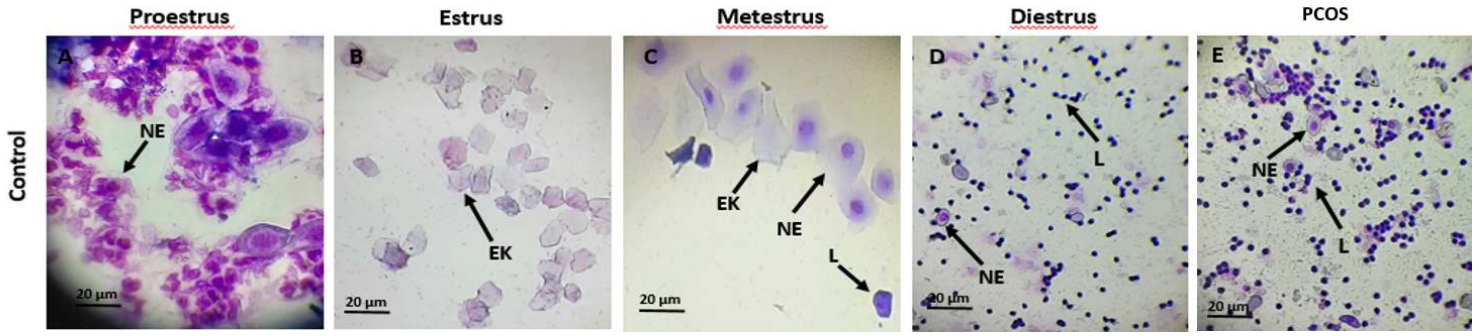

Figure 2

Representative photomicrographs of the four estrous stages. Identification of Proestrus by nucleated epithelial cells (NE), Estrous by cornified epithelial cells and keratinocytes (EK), Metestrus by nucleated cornified epithelial cells as well as a few leukocytes, and Diestrus by high numbers of leukocytes in the control group. Vaginal smears of PCOS rats showed predominantly leukocytes (L), the main cell types observed during the Diestrus stage.

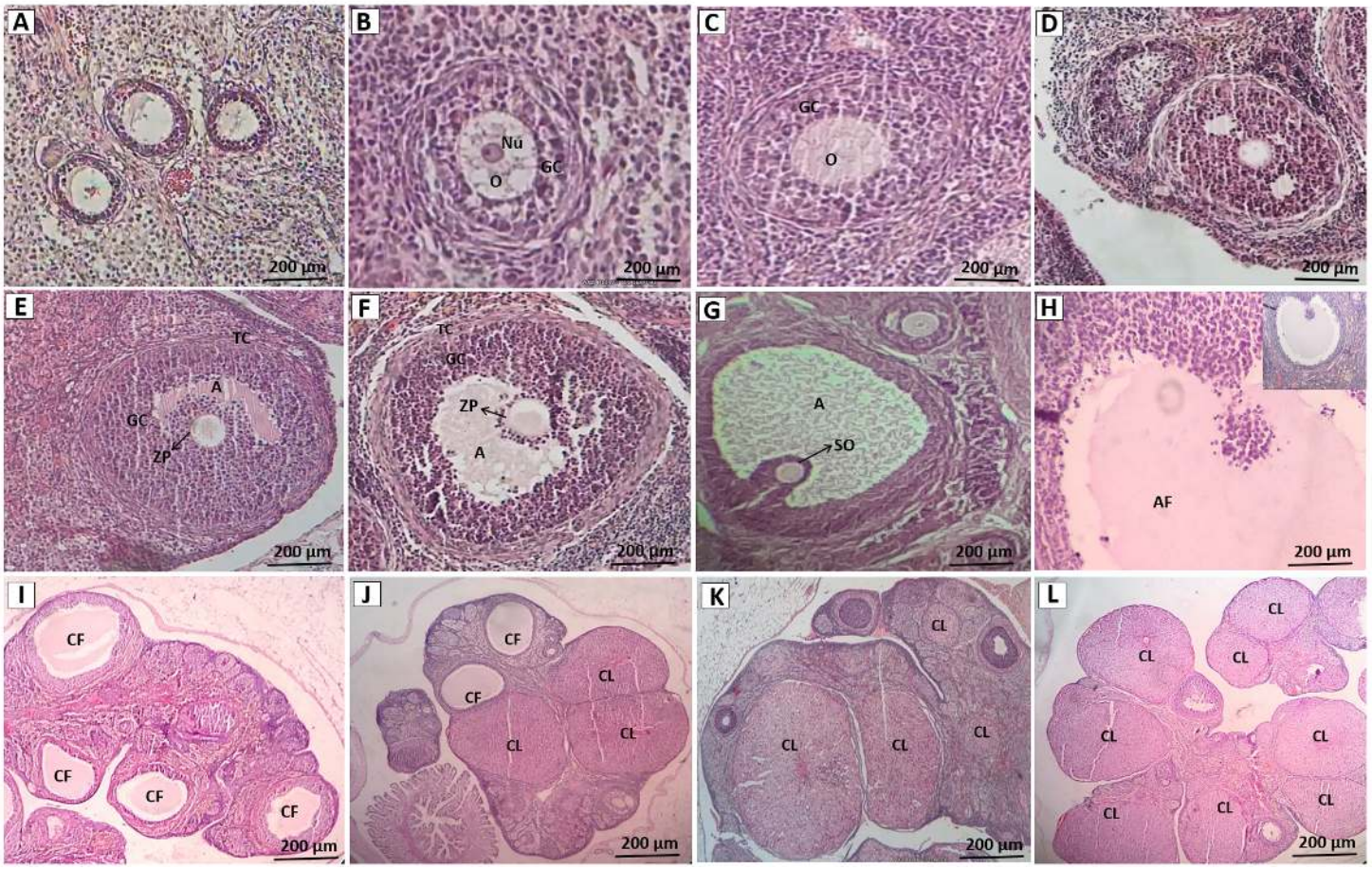

Figure 3

Histopathological representations of ovarian sections in the control and experimental groups. (**A-H**) The control group showed follicles at different developmental stages. (**A**) Primordial follicle. (**B**) Primary follicle. Nu, nucleus; O, Oocyte; GC, granulosa cells. (**C**) Pre-antral follicle. (**D**) Early-antral follicle. (**E**) Secondary follicle. A, antrum; ZP, zona pellucida; TC, theca cells. (**F**) Antral follicle. (**G**) Pre-ovulatory follicle. So, secondary oocyte. (**H**) Atretic follicle. (**I**) The ovaries of rats injected with EV developed cystic follicles with corpus luteum depletion. CF, cystic follicle. (**J, K, L**) The number of corpuses luteum increased after treatment with (**J**) 5 mg. (**K**) 10 mg and (**K**) 15 mg of Chn/Al-AH. CL, corpus luteum.

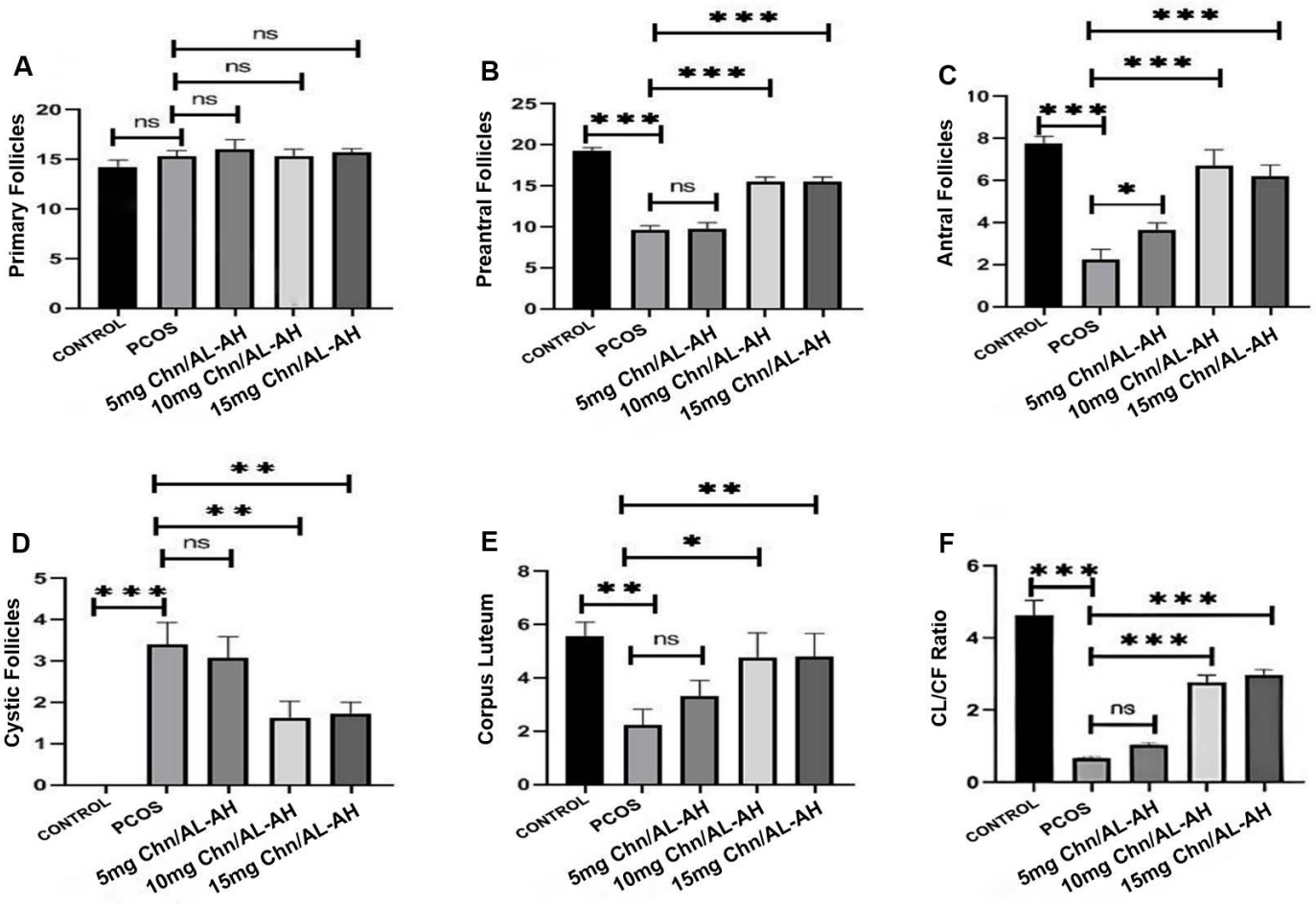

Figure 4

The numbers of follicles at different stages of development. (**A**) Primary. (**B**) Pre-antral. (**C**) Antral. (**D**) Cystic follicles. (**E**) Corpus luteum. (**F**) CL/CF ratio in different groups. Duncan's multiple range tests showed a significant difference in the mean value of each group (*P<0.05, **P<0.01, and ***P<0.001). ns represents not significant. Data are expressed as mean ± standard error (n=5).

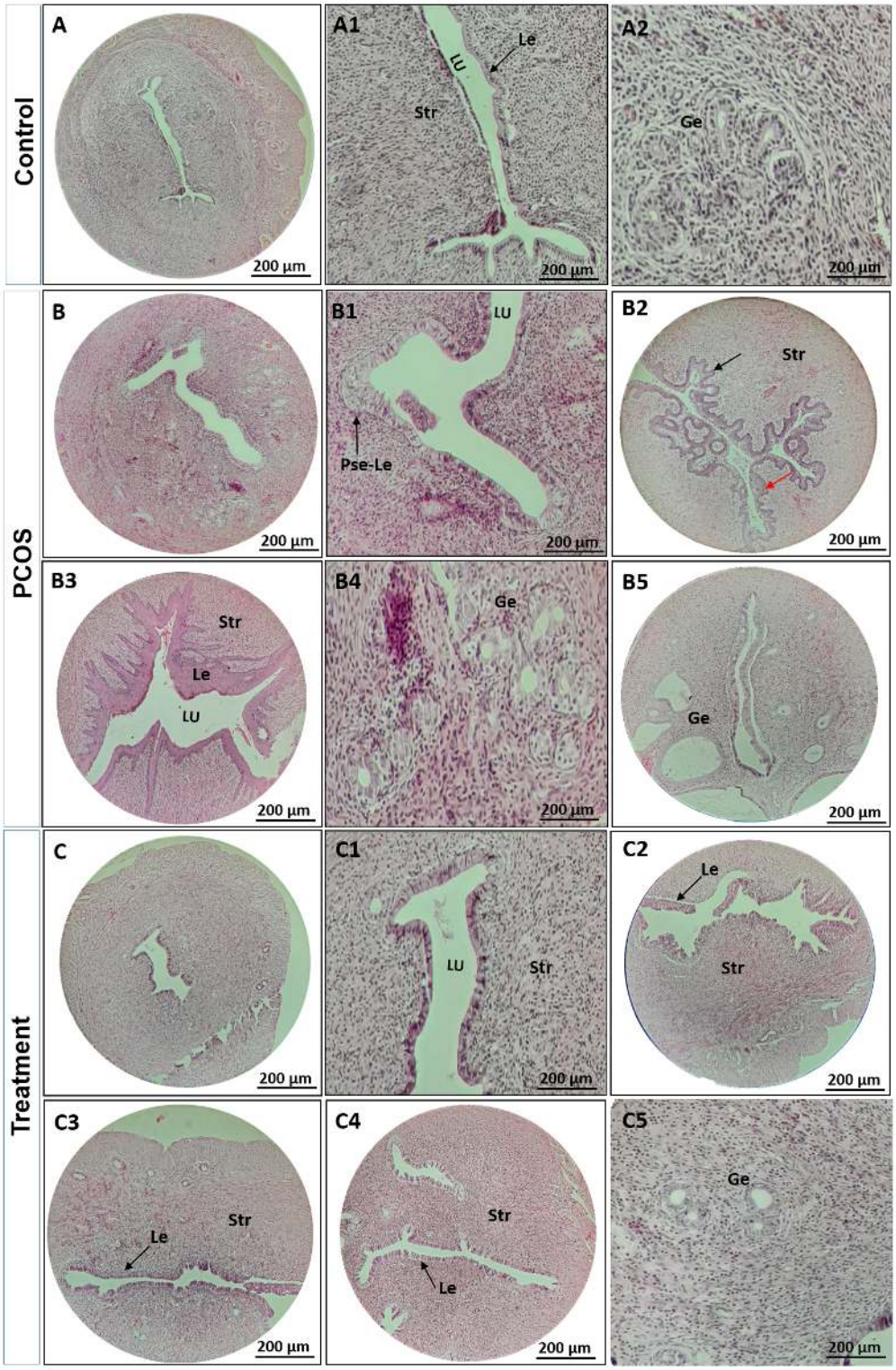

Figure 5

Photomicrographs of the representative uterine cross-sections. (**A**) Control. (**A1**) straight layer of columnar epithelium. Lu, lumen; Le, luminal epithelial cells; Str, stromal cells. (**A2**) single tubular uterine glands. Ge, glandular epithelial cells. (**B**) PCOS. (**B1**) Thickened columnar and pseudostratified epithelium. Pse-Le, Pseudostratified luminal epithelial cells (**B2**) Endometrial hyperplasia with cystic dilatation (black arrow) and convolution (red arrow). (**B3**) Endometrial hyperplasia with ciliated-shaped

cells in the stroma. (**B4**) conglomerate glandular epithelial cells. (**B5**) Cystic glands. (**C**) Treatment with Chn/Al-AH. (**C1**) Decreased thickness of epithelial cell layers. (**C2**) 5mg of Chn/Al-AH showed any improvement. (**C3**) 10 mg of Chn/Al-AH showed mild endometrial hyperplasia. (**C4**) 15 mg of Chn/Al-AH showed relative improvement in uterine morphology. (**C5**) Increased glandular epithelial cells.

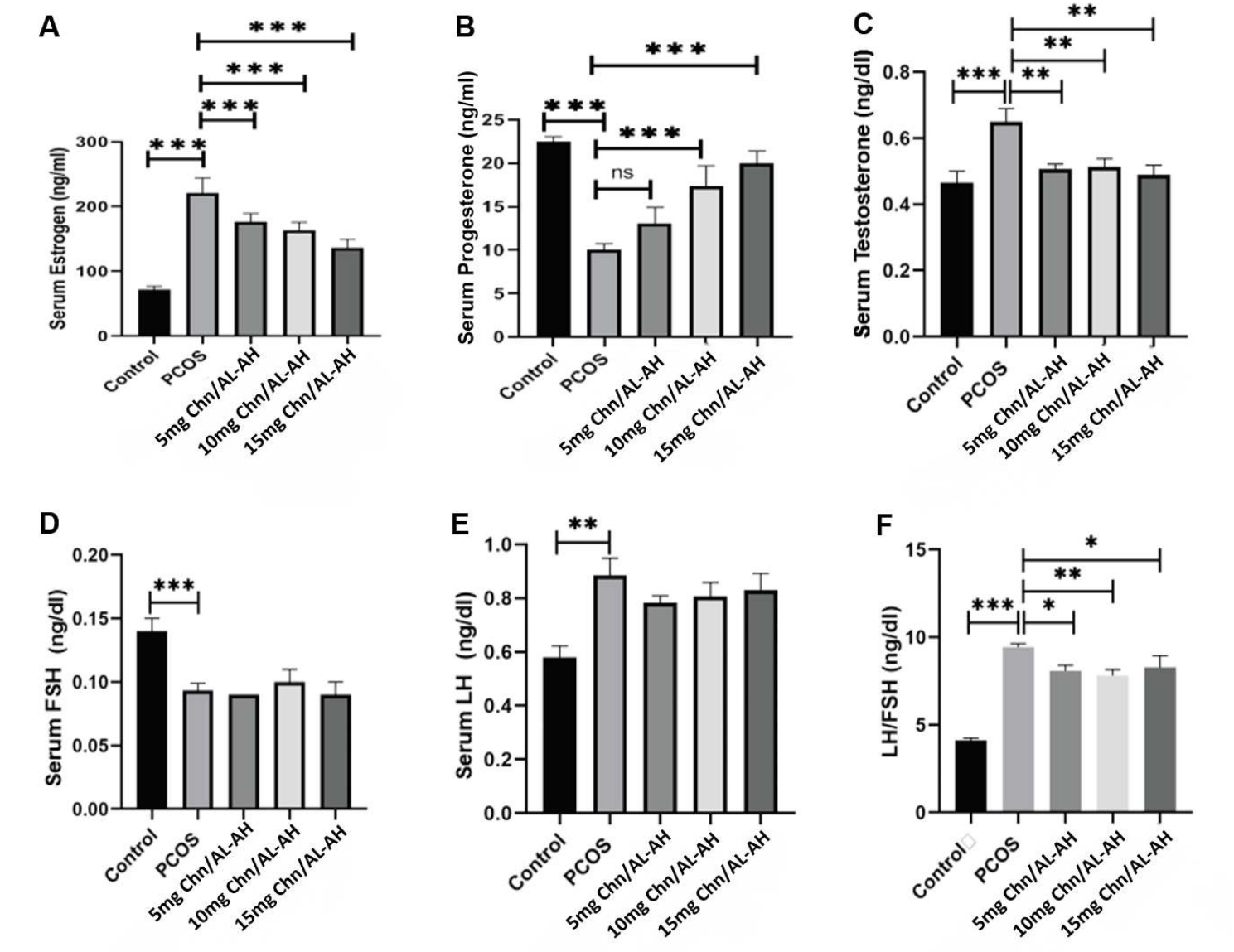

Figure 6

Reproductive hormone levels in different groups. (**A**) Estrogen. (**B**) Progesterone. (**C**) Testosterone. (**D**) FSH. (**E**) LH. (**F**) LH/FSH ratio. Duncan's multiple range tests showed a significant difference in the mean value of each group (*P<0.05, **P<0.01, and ***P<0.001) vs the PCOS group. Data are expressed as mean ± standard error (n=5).

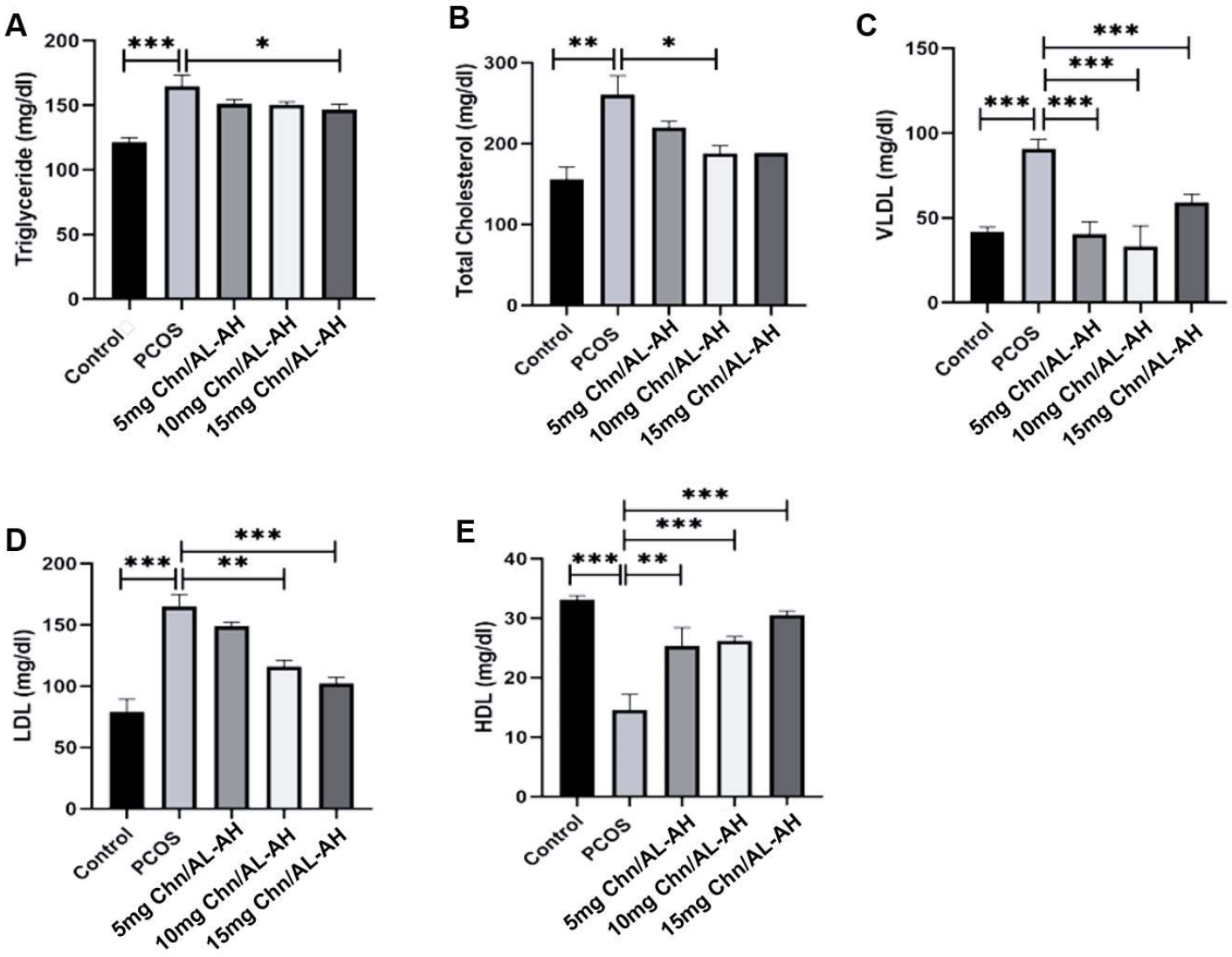

Figure 7

Comparison of serum lipid profile in different groups. (**A**) Triglyceride. (**B**) Total cholesterol. (**C**) VLDL. (**D**) LDL. (**E**) HDL. Duncan's multiple range tests showed a significant difference in the mean value of each group (n=5). *P<0.05, **P<0.01 and ***P<0.001 vs PCOS group. Data are expressed as mean ± standard error (n=5).

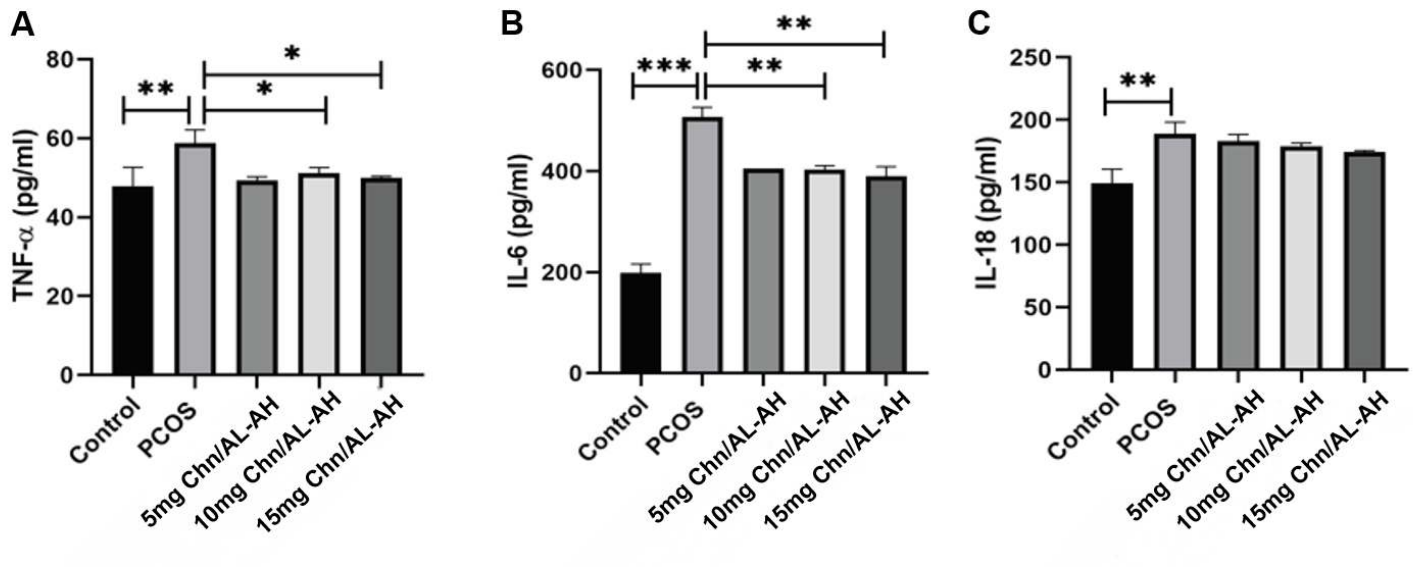

Figure 8

Serum levels of inflammatory markers in different groups. (**A**) TNF-α. (**B**) IL-6. (**C**) IL-18. Duncan's multiple range tests showed a significant difference in the mean value of each group (n=5)**.** *P<0.05, **P<0.01 and ***P<0.001 vs PCOS group. Data are expressed as mean ± standard error (n=5).

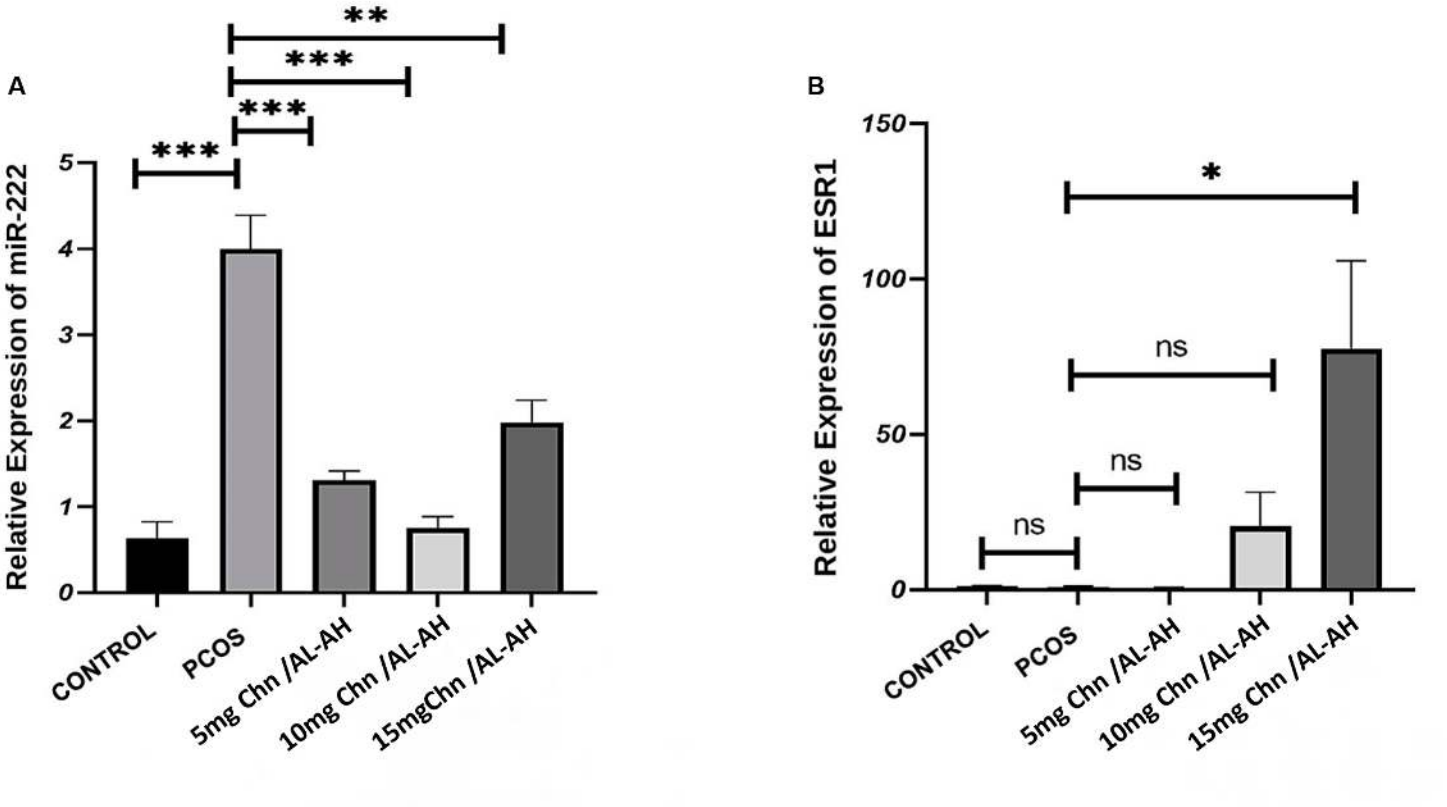

Figure 9

Relative expression of miRNA-222 and ESR1 in the PCOS and treatment groups. Duncan's multiple range test showed a significant difference in the mean value of each group (*P < 0.05, ** P < 0.01, and ***P < 0.001). ns represents not significant. Data are expressed as mean ± standard error (n=5).

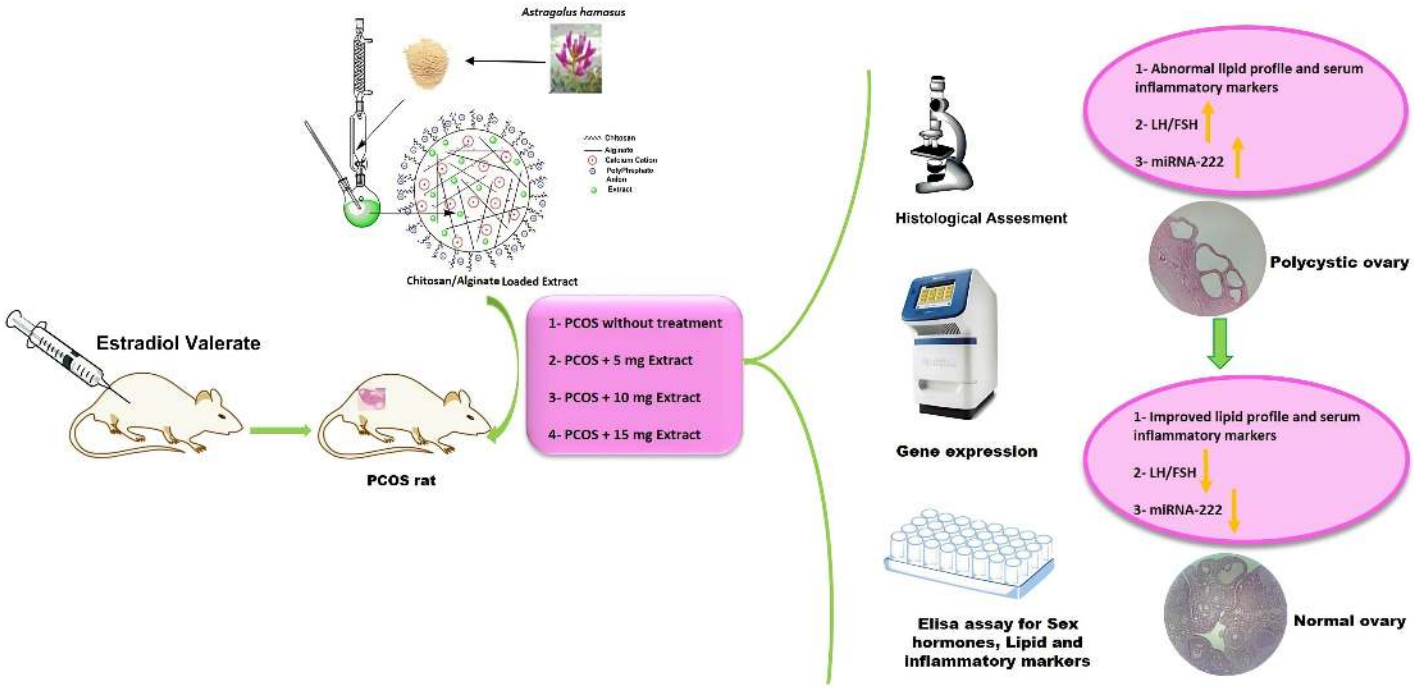

Figure 10

An overview of the workflow used in this study. PCOS was induced in rats by intramuscular injection of EV. PCOS rats were treated with three doses of chitosan/alginate hydrogel-loaded AH extract, including 5, 10, and 15mg/kg. The expression of miRNA-222 and ESR1, histopathology, and biochemical parameters were assessed.